Radio Science, Volume 33, Number 5, Pages 1361-1371, September-October 1998

Synthetic ΔK processing method applied to multifrequency radar observations

Eldar Aarholt

Teleplan AS, Defence Systems Engineering, Lysaker, Norway

Abstract. Both the range resolution and the range ambiguity interval of a sensor system can be maintained using a very much reduced number of data carriers across the bandwidth. This is demonstrated using real data from internal sea waves collected with a multifrequency radar system. The described signal processing methods favor the use of small numbers of sensors, which, through synthesis of additional data channels, give rise to a very high signal processing gain. Large synthetic sensor arrays can be constructed using very few real sensors for applications such as phased antenna array systems, microphone arrays for seismic prospecting, or imaging multifrequency radar systems.

1. Introduction

A new method to enhance the classification of radar targets by means of selective radar frequency and antenna distribution plans was presented by *Aarholt* [1996] using specific signal generating and processing methods involving the reconstruction of a large array of data channels using a smaller number arranged in the correct sequence, so that when the time series of each and every data channel is multiplied by the complex conjugate of the time series of the remaining data channels, additional data channels are synthesized. In the following, it will be shown that the method works using real data from a multifrequency radar system [*U.S.-Norway Ocean Radar Program*, 1995] probing wavenumbers from 0.002 m^{-1} to 0.5 m^{-1} to detect sea surface imprints of internally generated waves. The system is described in sufficient detail to allow for a direct comparison with a system using the new synthetic ΔK method.

The basic idea behind the ΔK radar system is that the half wavelength of the difference frequency between two carriers couples to structures of similar size; that is, a difference frequency of 10 MHz would couple to scatterers separated by approximately 15 m [$\Delta L = \lambda/2 = c/2\Delta F$]. As a consequence, more difference frequencies would allow correspondingly more reflector combinations to be probed. The transmitted radar carrier frequencies (upconverted intermediate-frequency K channels) are unevenly distributed according to a K channel frequency distribution plan which gives the position of each carrier. When combining two and two carriers (i.e., multiplying one channel by the complex conjugate of the other channel, as seen in equation (1)), the resulting difference frequencies are evenly distributed across the system bandwidth in accordance with

$$V_{\Delta F_m}(t) = V_{F_i}(t)\, V^*_{F_j}(t) \qquad (1)$$

$$i=1,n\text{-}1 \quad j=i+1,n \quad m=1,[n(n\text{-}1)/2]$$

where m is the number of ΔK data channels and n is the number of K data channels. An unwanted feature of this conventional ΔK channel generation method is the presence of "holes" in the ΔK frequency distribution when using more than four K channels. In this case, some of the array elements do not exist, and these are only represented with a value of zero, which leads to higher sidelobes in subsequent processing. The synthetic ΔK processing method uses two or more K channels to generate the ΔK channels. When permutating the above ΔK channels once more to a higher-order ΔK level [*Aarholt*, 1996], a large number of additional $S\Delta K$ channels [$k = m(m\text{-}1)/2$] will be generated using the following equation:

$$V_{\Delta\Delta F_k}(t) = V_{\Delta F_i}(t)\, V^*_{\Delta F_j}(t) \qquad (2)$$

$$i=1,m\text{-}1 \quad j=i+1,m \quad k=1,[m(m\text{-}1)/2]$$

Paper number 98RS01970.
0048-6604/98/98RS-01970$11.00

where k is the number of synthetic ΔK channels. This is equivalent to multiplying and permutating sets of four K channels. This process increases the number of channels probing the bandwidth as well as removes the unwanted holes in the ΔK frequency comb. The frequency plan is specified using an incremental frequency selection plan [*Aarholt*, 1996], in which the first K channel value is always zero. By adding each element in the incremental frequency plan, the selected frequency combination is generated. The resulting channels can be translated into any frequency band since waveform performance is only dependent on the difference frequency between the carriers.

2. The Multifrequency Radar System

The radar used was a coherent X-band multifrequency radar system equipped for the transmission of 32 simultaneous interrupted CW carriers from a circular aperture antenna of 0.9 m diameter [*Gotwols et al.*, 1996]. Power per carrier was about 400 mW, and the carriers were distributed over a 148.6-MHz bandwidth centered at 10.48 GHz [*U.S.-Norway Ocean Radar Program*, 1995].

The radar, located on a mountain site 820 m above sea level in the Sognefjord in Norway (61°14'N, 07°05'E), had separate horizontally polarized transmitter and receiver antennas, each with a beam width of 2.3° and a depression angle of 19.6°, which produced a footprint size of approximately 90 m in azimuth and 270 m in range on protected waters with a sea depth of 900 m. A schema drawing of the experiment can be seen in Figure 1. A total of 64 coherent (amplitude and phase) channels were recorded by the receiving system operating with fixed gain and achieving a dynamic sampling range of 90 dB (15 bit).

The frequency plan used was designed to provide equally spaced difference frequency wavelengths to match the expected length scales of the internal wave patterns (15 m to 80 m) as imaged on the sea surface, as well as to cover length scales of surface waves (1 m to 4 m), which may also be directly modulated by the internal wave currents. The frequency plan consisted of two frequency bands, each with 16 frequencies. Within each 16-frequency band, the lower eight frequencies were separated by $\Delta f = 0.63585$ MHz, the next seven frequencies were separated by $9\Delta f$, and the highest frequency was separated by $8\Delta f$. The frequency gap between the two bands, $78\Delta f$, is filled with channels through the ΔK process. Figure 2 shows the intermediate-frequency distribution of the 32 frequency synthesizers used by the radar system. The difference frequencies are obtained by subtracting pairs of frequencies within the upper and the lower band, normalized to the fundamental separation of 0.63585 MHz. A total of 234 unique equally spaced ΔK channels without holes are generated using this carrier distribution out of a total of $n(n\text{-}1)/2 = 32(32\text{-}1)/2 = 496$ possible combinations. This distribution also gives rise to a number of replicated ΔK channels which may be coherently averaged.

The internal wave action, which can best be seen in Sun glitter from an elevated position such as from the radar site, is produced in layers having high temperature, density, and/or salinity gradients. Currents generated by the internal wave modify the surface wave spectrum by Doppler shifting energy from one part to another, thereby introducing a modulation of the radar scattering cross section as a function of the internal wave phase.

It is worth noting that the carrier distribution seen in Figure 2 was selected to give full ΔK-channel coverage across the available bandwidth for a radar system using conventional ΔK radar processing methods; in this context it acts as a constraint and is not an optimal configuration to demonstrate the synthetic ΔK frequency concept. However, by thinning the 32 carriers used in the above setup to 12, the very same 234 unique equally spaced ΔK channels can be constructed using the synthetic ΔK method. This allows for the use of both the same data file for conventional and synthetic ΔK processing and the same signal processing code, with the exception of a modified subroutine generating the synthetic ΔK data set. The selected carrier distributions for the two methods are listed in Table 1.

The frequency plan for the n=32 carrier radar system was divided into two identical 15-element incremental frequency plans (1, 1, 1, 1, 1, 1, 1, 9, 9, 9, 9, 9, 9, 9, 8), both of which were concatenated and separated by 78 channel positions. The synthetic ΔK method reduces the number of required frequencies to n=12, and the subsequent "11-element" incremental frequency plan becomes (4, 1, 2, 18, 36, 9, 8, 78, 34, 27, 17). Both frequency plans generate 234 equally spaced ΔK channels without holes.

When using the 11-element synthetic ΔK incremental frequency plan above, the maximum number of ΔK channels would be m=66 from equation (1) using n=12 K channels. By permutating these 66 ΔK channels once more to a higher-order ΔK level, an additional $66(66\text{-}1)/2 = 2145$ $S\Delta K$ channels will be generated using equation (2). To illustrate the process, a simple analog representation of the signal flow in a four-channel synthetic ΔK sig-

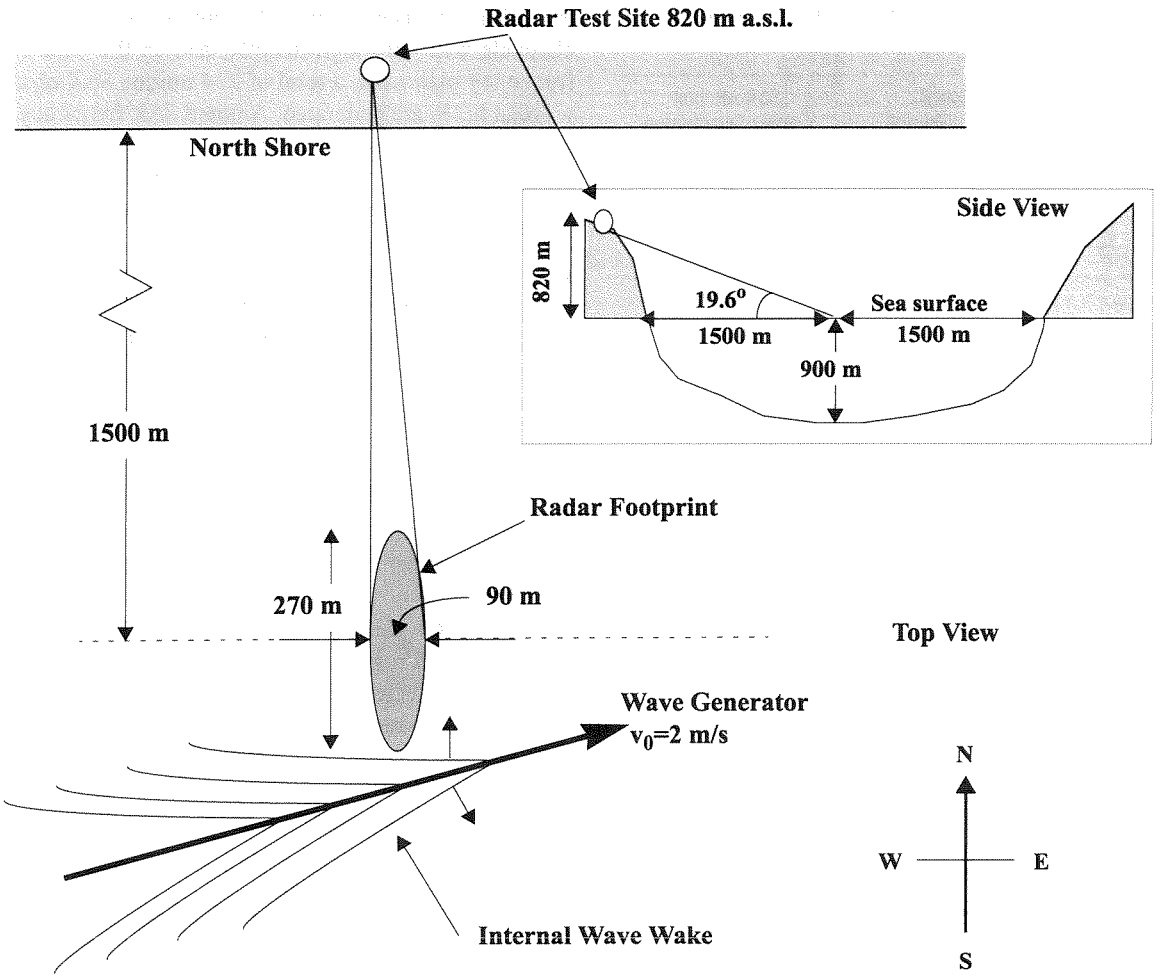

Figure 1. The experiment was located about 150 km from the North Sea in Sognefjord in Norway. A deep-draft surface vessel was used to inject energy into the upper layered structure of the fjord, and the surface signature of internal waves generated by the vessel was monitored by radar systems on the mountain side.

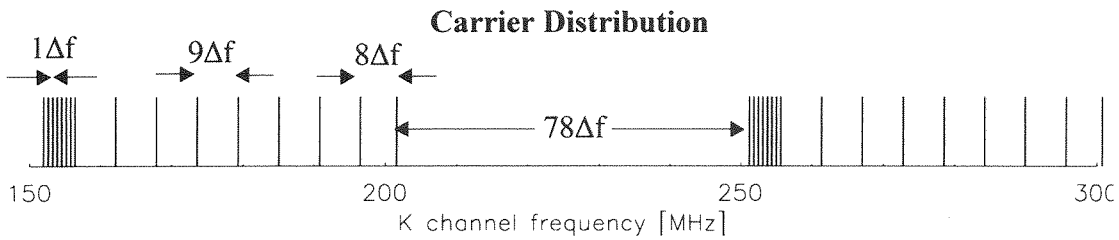

Figure 2. The radar system intermediate-frequency synthesizers are distributed from 150 to 300 MHz and upconverted to the 10-GHz frequency band. Each vertical line denotes the relative carrier frequency position. The smallest frequency difference is Δf=0.63585 MHz.

Table 1. Conventional ΔK and Thinned $S\Delta K$ Carrier Distribution

K Channel Number	ΔK Method Carrier Distribution $V_F(t)$	$S\Delta K$ Method Carrier Distribution $V_F(t)$
K_1	0	0
K_2	1	...
K_3	2	...
K_4	3	...
K_5	4	4
K_6	5	5
K_7	6	...
K_8	7	7
K_9	16	...
K_{10}	25	25
K_{11}	34	...
K_{12}	43	...
K_{13}	52	...
K_{14}	61	61
K_{15}	70	70
K_{16}	78	78
K_{17}	156	156
K_{18}	157	...
K_{19}	158	...
K_{20}	159	...
K_{21}	160	...
K_{22}	161	...
K_{23}	162	...
K_{24}	163	...
K_{25}	172	...
K_{26}	181	...
K_{27}	190	190
K_{28}	199	...
K_{29}	208	...
K_{30}	217	217
K_{31}	226	...
K_{32}	234	234

Table shows the thinned carrier distribution used by the synthetic ΔK system compared with a conventional ΔK system.

nal processing unit is included in Figure 3. These calculations result in a total of 66 + 2145 = 2211 possible ΔK channels, and in a signal processing sense, the ΔK and the $S\Delta K$ channels are treated equally. Depending on the initial frequency plan, the number of unique $S\Delta K$ channels will vary significantly, and in the case of the frequency plan used, a total of 234 unique $S\Delta K$ channels without holes are generated. A tuned $S\Delta K$ frequency plan using 12 carriers would improve channel distribution up to of the order of 1500 unique equally spaced $S\Delta K$ channels and improve the signal processing gain by 20 log(1500/234) = 16 dB compared with the processed data set. However, the number of channels was limited by the 148.6-MHz radar bandwidth and the 0.63585-MHz minimum channel frequency separation used in the experiment.

3. $S\Delta K$ Image Processing of Internal Wave Measurements

In order to demonstrate the application of the method in radar systems, a well-documented data set from radar measurements of internal waves generated by a surface vessel is used [*Gotwols et al.*, 1996]. The US-Norway Ocean Radar Program field test in 1995 [*Gasparovic et al.*, 1995] collected data from a total of 31 surface runs and involved participation of the Johns Hopkins University Applied Physics Laboratory, the Defence Research Agency UK, the Royal Norwegian Navy, the Norwegian Defence Research Establishment, the Environmental Surveillance Technology Programme (P.F.M.), and the company Susar in Norway.

Data from 32 and 12 carriers were used to generate the 234 ΔK and $S\Delta K$ channels, respectively (see Table 1). The wake images seen in Figure 4 show conventional (Figure 4a) and synthetic (Figure 4b) ΔK processing obtained by the following steps: (1) The sampled time series phase was calibrated, and (2) the equal ΔK and $S\Delta K$ channel timeseries were averaged coherently. (3) One data sample from each time series was selected to construct an array consisting of 234 samples. (4) A second phase calibration and a (5) Hanning window were applied to the array while (6) zero-padding the data array to 512 elements. The final step was to compute the fast Fourier transform (FFT) to obtain the range profile from the data set. This process was repeated for each individual time sample. The resulting frequency spectra were averaged every 5 s, and the magnitude was plotted using a color-coded logarithmic scale (in decibels). The constructed image records the wave propagating through the antenna footprint. The range interval ($\Delta Z = c / (2\Delta F_{min})$ = 235 m) originates from the half wavelength of the lowest ΔK channel frequency (ΔF_{min} = 0.63585 MHz). The bandwidth used (ΔF_{max} = 148.6 MHz) gives the radar

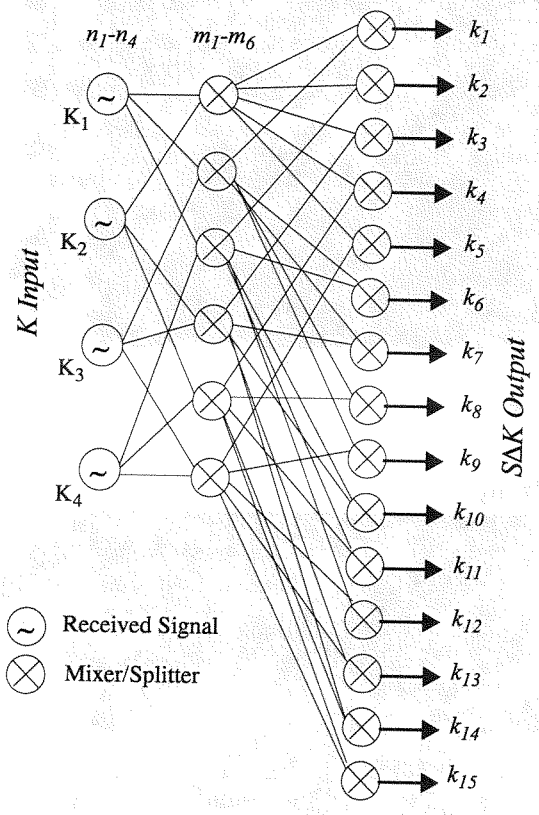

Figure 3. An analog representation of the signal flow in a four-channel synthetic ΔK signal processing unit.

resolution ($\Delta z = c / (2\Delta F_{max}) = 1.0$ m). Multiple clear wake structures can be seen in the images. The slope dz/dt of the wake gives the maximum phase velocity v_o = 0.65 m/s of the internal wave. This is in agreement with theoretical calculations, observations, and experimental data. The synthetic ΔK image is similar to the one generated using the full data set, apart from a degradation of the signal-to-noise (S/N) ratio as seen in the synthetic ΔK image.

3.1. First Noise Considerations

The signal-to-noise ratio for the experimental setup can be calculated with reference to *Alpers and Hasselmann* [1978], such that

$$\text{S/N ratio} = 0.1\left(\frac{\hat{\lambda}}{2x_0}\right)^2 \sqrt{2}\left|\frac{\boldsymbol{k}}{\Delta \boldsymbol{k}}\right| \tag{3}$$

where the wavenumbers are $|\mathbf{k}| = 2\pi/0.03$ m^{-1} (X band) and $2\pi/472$ m^{-1} < $|\Delta\mathbf{k}|$ < $2\pi/2$ m^{-1}; $\hat{\lambda}$ is the internal wake wavelength (typically 60 m); and x_0 is the horizontal projection of the antenna footprint (x_0 = 270 m) using a depression angle of 19.6°. From Figure 5 it is seen that the potential S/N ratio is highest for the longer wavelengths. It must be noted that the only difference between the conventional and the synthetic ΔK generation is an additional complex multiplication, such that

$$S\Delta K = \Delta K_i \; \Delta K_j \tag{4}$$

Fundamental to the ΔK and the $S\Delta K$ process is the use of a complex multiplier to correlate the available K channels and produce the $S\Delta K$ channels. Since the S/N ratio of each input to these multipliers is finite, the loss in the S/N ratio imposed by such a multiplier must be explored. The analogy in this context is that of a mixer which has one variable S/N ratio input and one high S/N ratio input, commonly referred to as the local oscillator. The output noise arises from $N_j x S_i$, $N_i x S_j$ and $N_i x N_j$. The derived formula shows that the S/N ratio out of the multiplier is related to the two inputs in accordance with

$$\frac{P_i \; P_j}{1 + P_i + P_j} \tag{5}$$

where P_i and P_j are the S/N ratio (power) of the inputs as seen in Figure 6. In practice, the S/N ratio of each input to the multiplier is near identical, since the signal and noise levels are not expected to vary much between individual carriers. Note that the two input signal ratios are measured in the bandwidth in which the multiplier is operating. This implies that the multiplier should be operated at a low bandwidth to minimize loss.

When multiplying two complex signals at high input S/N ratios, the signal degradation is only 3 dB; that is, multiplying two channels (conventional ΔK) reduces the S/N ratio by 3 dB, and multiplying four channels reduces it by 6 dB, which is equivalent to equation (4). For very low input S/N ratios (effectively <1), the degradation is essentially squared. The S/N ratio difference between the

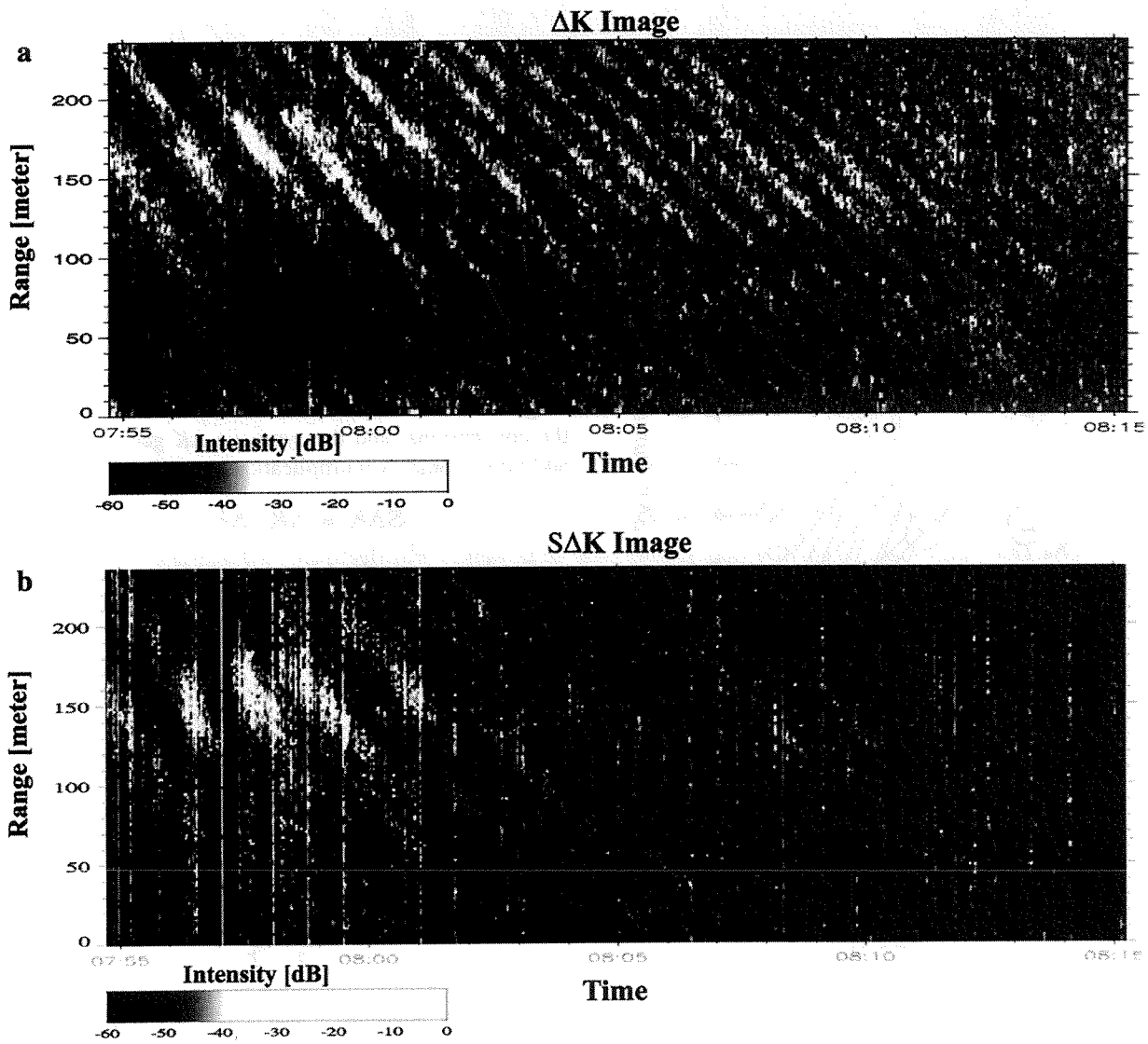

Figure 4. The constructed image records the wave propagating through the antenna footprint toward the radar system. Shown are results of (a) the conventional ΔK signal processing and (b) the synthetic ΔK processing method. It is seen that the wake arms are strongest during the first few minutes of the measurement.

ΔK and the $S\Delta K$ method is therefore -3 dB for S/N ratio >1, increasing to -6 dB for lower S/N ratios. To reach a quantitative experimental estimate for the loss in the above example, a time slice of the received power across the internal wave image can be seen in Figure 7 for the internal wave data set using all 32 carriers (Figure 7a) and the thinned 12-channel synthetic ΔK carrier selection (Figure 7b). It is seen that the absolute spectral amplitude is of the order of 4 dB lower when using the synthetic ΔK processing method, while the S/N ratio is comparable during the first few minutes of the measurement. In both cases, the internal waves are easily detectable with a S/N ratio of 10-15 dB for the first five wake arms of the measurement. In the case when all available carriers are used, more wake arms are seen later in the image. This indicates that the available dynamic range in the data set has been reached due to the multiplicative loss for the synthetic ΔK processing. The digitized signal from the sea

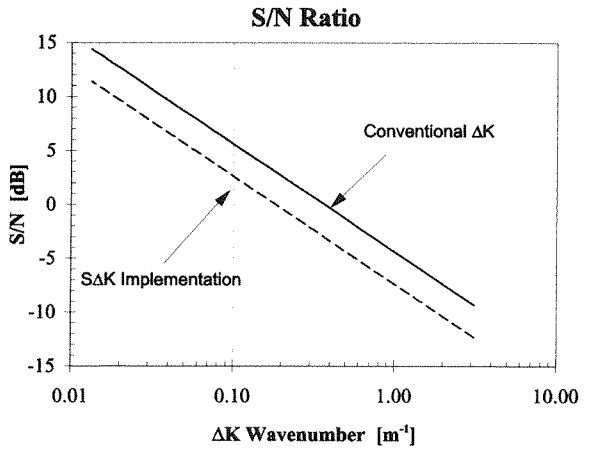

Figure 5. The internal wave experiment signal-to-noise (S/N) ratios as a function of wavenumber.

clutter had a maximum dynamic range (full scale deflection) of 48-55 dB throughout the measurement, which was adequate to detect internal waves above a threshold intensity. From this, it is evident that the initial S/N ratio is sufficiently high to accommodate the increased multiplicative loss imposed by the synthetic ΔK processing method. As a consequence, the required radar hardware can be reduced significantly.

3.2. Matched Filter Processing

The internal wave behaves according to certain known principles [*Dysthe and Trulsen*, 1989]. The radar Doppler return from hard targets varies linearly with velocity, while for ocean waves, the Doppler varies as a function of the dispersive nature of the wave. The dispersion relation [*Barber*, 1993] for an internal wave seen by the radar is

$$\text{Dispersion} = \left(\frac{1}{\left(\frac{v_{\text{phase}} 2\Delta F \cos(\theta)}{c} \right)} + \frac{1}{\omega_{bw}} \right)^{-1} \text{Hz} \quad (6)$$

where v_{phase} is the phase velocity, ω_{bw} is the Brünt-Väisälä frequency, θ is the radar antenna depression angle, c is speed of light, and ΔF is the radar difference frequency. Typical values of these variables are v_{phase} = 0.65 m/s, ω_{bw} = 0.0398 Hz, θ = 19.6°, $c = 3 \times 10^8$ m/s, and the difference frequency was 0.635 MHz < ΔF < 148.6 MHz. Inserting these values into equation (6) gives the dispersion relation seen in Figure 8. This a priori information can be used to construct a filter which would enhance the signal resulting from the internal wave action and suppress the sea clutter [*Gjessing*, 1986]. It

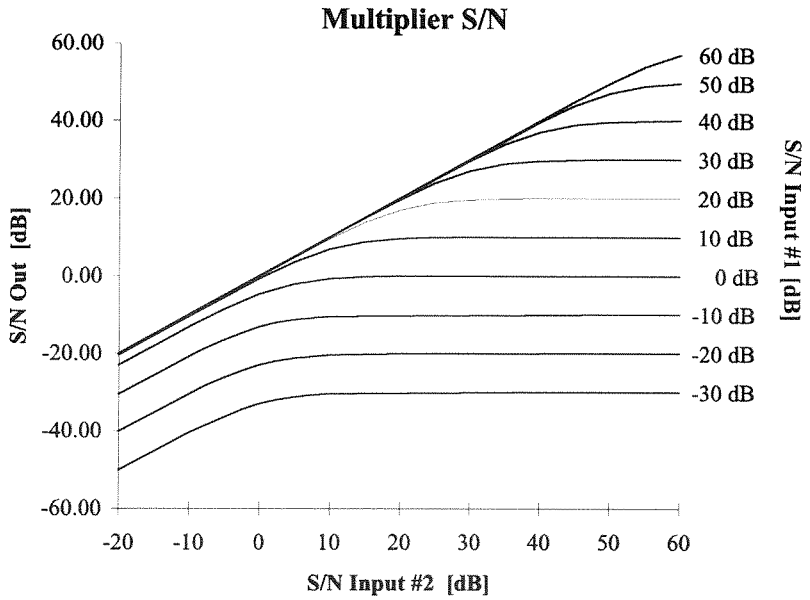

Figure 6. The S/N ratio output level when multiplying two complex signals for several S/N ratio levels.

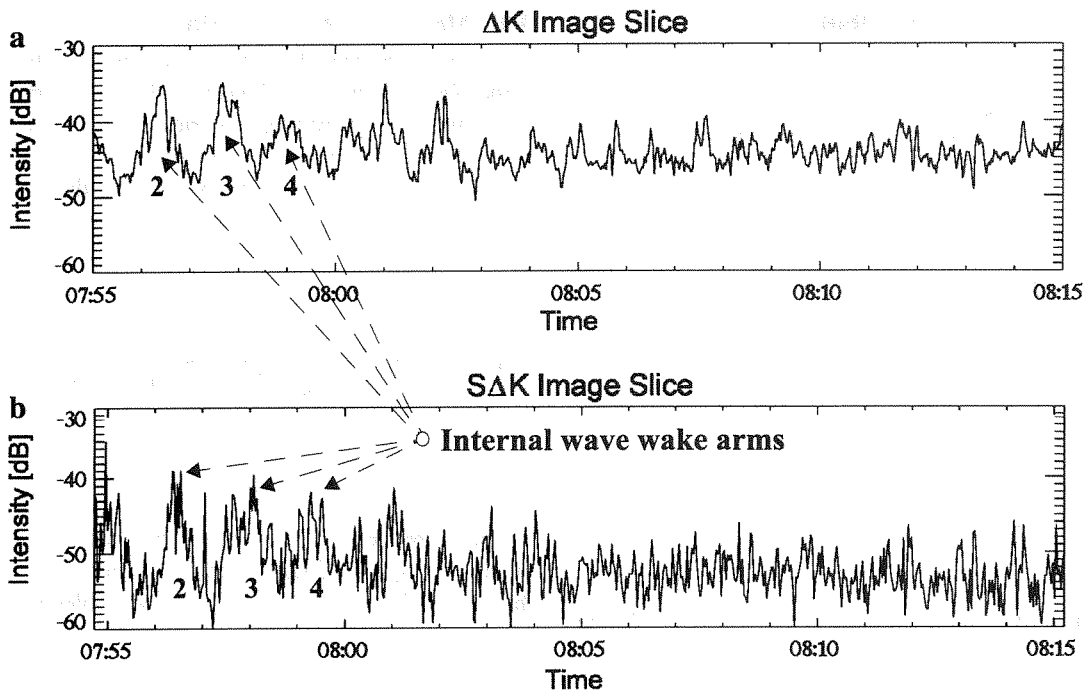

Figure 7. A time slice of the received power across the internal wave image at range interval position 150 m using (a) the conventional ΔK signal processing method and (b) the synthetic ΔK processing method. The absolute power is about 4 dB higher when using all available carriers, while the S/N ratio is comparable for the four numbered wake arms.

will now be shown that matched filters can be used on a system using the synthetic ΔK processing method.

Figure 9 shows the internal wave activity when summing all the frequency components of the synthetic ΔK channels below 20 MHz (possessing channels with the highest potential S/N ratio, as seen in Figure 5) after first shifting the received ΔK channel time series by a frequency $e^{-j\Delta\omega t}$. This corresponds to the shift $\Delta\omega$ of the expected internal wake dispersion relation for each ΔK channel frequency seen in Figure 8. The resultant frequency shift (Doppler) produced by the internal wave velocity would therefore be 0 Hz for all frequency-shifted ΔK channels, and the internal wave response should therefore appear around zero Doppler. The resulting spectra are subsequently averaged. On the basis of this experience, this is a very robust and powerful means of detecting the internal wave clearly seen during the first 5 min of the measurement. This agrees very well with the internal wave images shown in Figures 4 and 7. This filter enhances a dispersive target, producing a Doppler frequency according to Figure 8, and similarly, any zero-Doppler target would be smeared out in frequency along the Doppler frequency curve in Figure 8, but with a negative sign. The velocity of a gravity wave would produce a Doppler frequency about 10 times higher in frequency than that of an internal sea wave and would therefore not appear in the matched filter output.

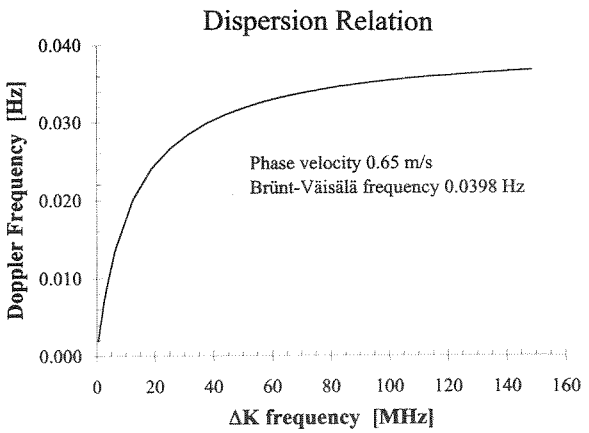

Figure 8. The internal wave dispersion relation calculated using equation (3) and with appropriate radar operating parameters. The calculated frequency data are used to construct a matched filter for the internal wave.

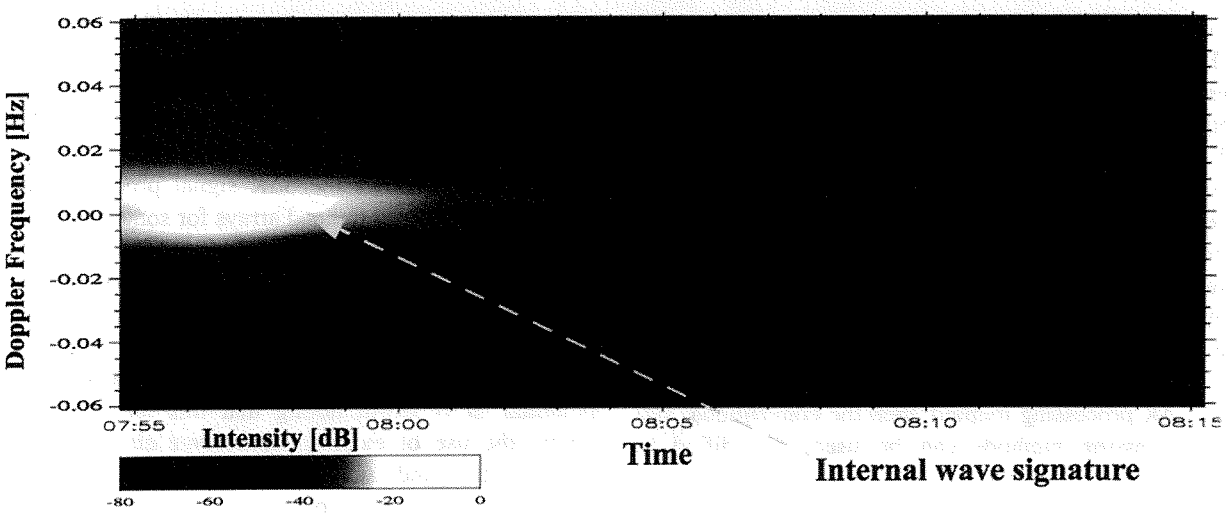

Figure 9. Dispersion shifted ΔK radar data based on the synthetic ΔK processing method showing the mean spectral return of all ΔK channels below 20 MHz. A strong internal wave is seen during the time period 0755-0800 UT.

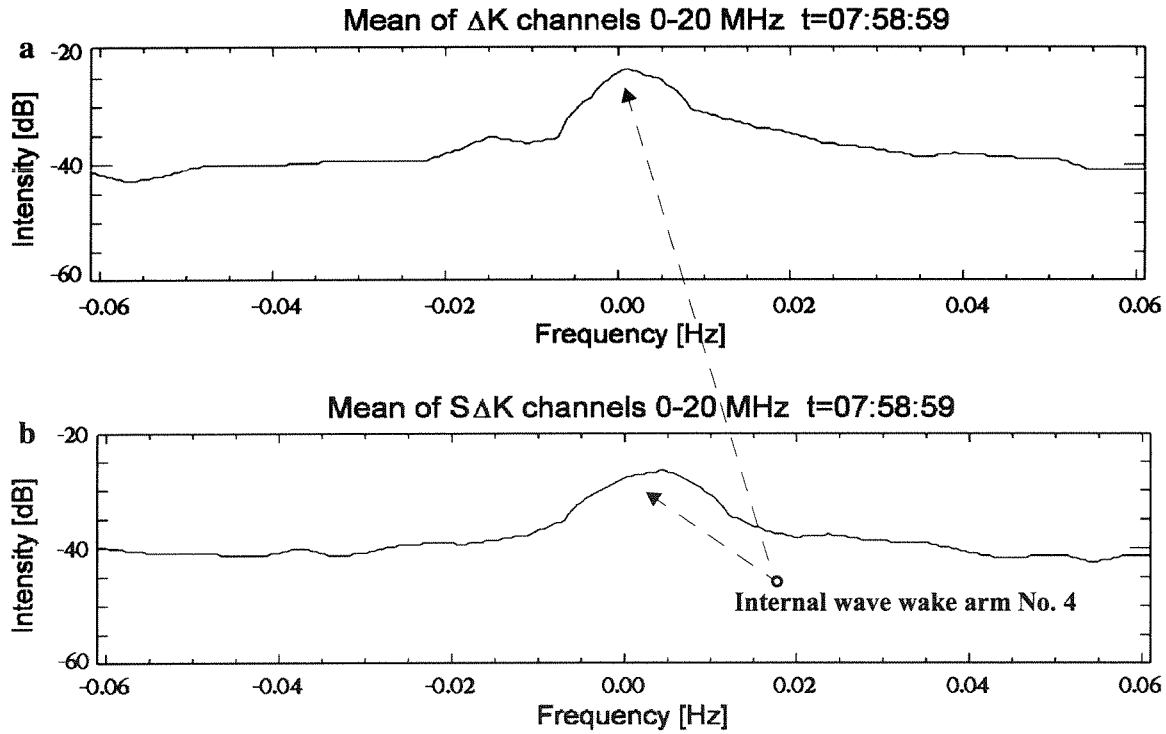

Figure 10. A time slice of the received power across the internal wave image using (a) the conventional ΔK signal processing method and (b) the synthetic ΔK processing method. The absolute power and the S/N ratio are about 5 dB higher when using all available carriers.

3.3. Second Noise Considerations

Figure 10 shows a frequency spectrum slice across the mean of the dispersion relation shifted internal wave ΔK frequency spectra seen in Figure 9 at time mark 0758:59 UT using all 32 carriers (Figure 10a) and the thinned synthetic ΔK carrier selection (Figure 10b). The data represent wake arm number 4 seen in Figures 4 and 7. It is seen that the maximum spectral amplitude and the S/N ratio are about 5 dB lower when using the 12-carrier synthetic ΔK processing method. Again, it is evident that if the initial S/N ratio is sufficiently high to accommodate the increased multiplicative loss imposed by the synthetic ΔK processing method, then the conventional signal processing methods can be used unmodified to further enhance and characterize the object of interest.

4. Related Applications Phased Antenna Arrays and Seismic Microphone Arrays

The synthetic ΔK method can be used in several widely different technologies, and since the radar application may be unfamiliar to the reader, some other applications are suggested in the following.

The theory can be applied to phased antenna array systems and seismic microphone arrays, reducing the required hardware by orders of magnitude and consequently the system's real-time data rate. The data synthesis is performed using a two-dimensional synthetic sensor distribution [*Aarholt*, 1996] and the digital signal processing algorithms given in equations (1) and (2). The method would significantly reduce the complexity, weight, and cost of antenna arrays without seriously degrading antenna performance. The loss in the signal-to-noise ratio resulting from the two-dimensional synthetic ΔK computations is, with reference to section 3.1, of the order of 12 dB (twice that of a one-dimensional array). Table 2 shows the $S\Delta K$ signal processing gain improvement over unthinned arrays for some array sizes, taking the gain reduction imposed by the multiplicative loss into account. It is seen that the method becomes increasingly more attractive by adding a few real elements in the synthesis, resulting in millions of synthetic elements and a considerable signal processing gain potential. It is worth noting that this implementation favors the use of existing transceiver circuitry, phase compensation, and sampling hardware and software. The modification acts as a computational subroutine which reconstructs the full sensor matrix to which existing signal processing algorithms can be applied.

5. Conclusions

This paper demonstrates that both the range resolution and the range ambiguity interval can be maintained using a very much reduced number of data carriers across the bandwidth in a sensor system. The synthetic ΔK signal processing method favors the use of small numbers of sensors, which through digital data synthesis give rise to a very high signal processing gain. Very large synthetic sensor arrays can be constructed using very few real sensors. It is important to bear in mind that a sufficiently large number of real data carriers must be used to resolve more complex structures in the target of interest.

Table 2. $S\Delta K$ Signal Processing Gain Improvement Over Unthinned Arrays

Real		Synthetic					
Number of Real Elements n_R	Signal Processing Gain, dB $G_R = 20\log(n_R)$	Number of Synthetic Elements n_S	Signal Processing Gain, dB $G_S = 20\log(n_s)$	Multiplicative Loss, dB L_M	Total Signal Processing Gain, dB $G_T = G_S - L_M$	Equivalent Real Element Array Size n_{ER}	Total Signal Processing Gain Improvement, dB $G_I = G_T - G_R$
6x6	31.1	42x42	64.9	-12	52.9	21x21	21.8
8x8	36.1	115x115	82.4	-12	70.4	57x57	34.3
12x12	43.1	1,500x1,500	127.0	-12	115.0	750x750	71.9
20x20	52.0	10,000x10,000	160.0	-12	148.0	5,011x5,011	96.0

Table shows the number of real and synthetic elements, as well as the corresponding signal processing gains for some array sizes (gain = 20 log(number of elements)). The total signal processing gain is equivalent to that of an unthinned real element antenna array size (n_{ER}), that is, the number of elements constituting a signal processing gain of G_T ($n_{ER} = 10^{(G_T/20)}$). The total signal processing gain improvement imposed by the method is also shown. A phased array system has one signal source which is divided between all elements. Reducing the number of transmitter elements by thinning increases the power of each transmitter element accordingly. Therefore the transmitter power does not enter the calculations.

The addition of just a few more real sensors in a synthetic array system would improve the signal budget to a great extent since the multiplicative noise would remain constant while the number of synthetic sensor elements would increase exponentially. The method does not favor applications operating to the limit of signal detection capability but has its highest potential in applications with a positive S/N ratio after initial signal integration, in which case an improved signal processing gain is achieved. When compared with conventional systems and methods, the required sensor hardware and data rate can be reduced by a factor of 10-1000.

Acknowledgments. The experimental work was carried out during my affiliation with the Environmental Surveillance Technology Programme (P.F.M.) and the company Susar AS in 1995 as part of the U.S.-Norway Ocean Radar Program 1988-1995. I would like to express my thanks to P.F.M. for the use of signal processing equipment, thereby allowing me to pursue my research activities. I am also very grateful to Alexander S. Hughes at the Johns Hopkins University Applied Physics Laboratory, in Laurel, Maryland, for valuable discussions and encouragement over several years.

References

Aarholt, E., Synthetic ΔK frequency plans in relation to radio wave object characterization, *Radio Sci.*, 31(4), 841-857, 1996.

Alpers, W., and K. Hasselmann, The two-frequency microwave technique for measuring ocean-wave spectra from an airplane or satellite, *Boundary Layer Meteorol.*, 13, 215-230, 1978.

Barber, B. C., On the dispersion relation for trapped internal waves, *J. Fluid Mech.*, 252, 31-49, 1993.

Dysthe, K. B., and J. Trulsen, Internal waves from moving point sources, *JHU-APL Tech. Dig.*, 10(4), Appl. Phys. Lab., Johns Hopkins Univ., Laurel, Md., 1989.

Gasparovic, R. F., A. S. Hughes, and R. D. Chapman, U.S.-Norway Ocean Radar Project, 1995 Sognefjord Experiment Test Operations Plan, *Rep. JHU/APL SIR-95-09*, 42 pp., Appl. Phys. Lab., Johns Hopkins Univ., Laurel, Md., June 1995.

Gjessing, D. T., *Target Adaptive Matched Illumination Radar, IEE Electromagn. Waves Ser.*, vol. 22, 172 pp., Peter Peregrinus, London, 1986.

Gotwols, B. L., E. Aarholt, R. D. Chapman, and R. E. Sterner II, Optical, radar and in-situ measurements of internal wave dispersion, in *Proceedings of the 1996 International Geoscience and Remote Sensing Symposium*, IEEE Cat. No. 96CH35875, vol. III, pp 1736-1738, 1996.

U.S.-Norway Ocean Radar Program 1995, Advanced Sensor Applications - ΔK Technique Project, *Rep. PFM/Susar/Triad*, 200 pp., Dep. U, Norw. Def. Res. Estab., Horten, Norway, November 1995.

E. Aarholt, Teleplan AS, Fornebuveien 33-35, P.O. Box 69, 1324 Lysaker, Norway. (e-mail: aar@teleplan.no)

(Received October 24, 1997; revised May 21, 1998; accepted June 11, 1998.)